

# EFFECT OF JUNCTION CELL TEMPERATURE AND GEOGRAPHICAL COORDINATES ON THE ELECTRICAL PERFORMANCES OF A PHOTOVOLTAIC MODULE

C. BOUTGHAN<sup>1,\*</sup>, O. KHOLAF<sup>2</sup>, S. BENATTALAH<sup>1</sup>

<sup>1</sup>Faculty of the exact sciences, laboratory of Energetic Physics, Mentouri Brothers University, Constantine 1, Algeria

<sup>2</sup>Department of Transport Engineering, Mentouri Brothers University, Constantine 1, Algeria

\*Corresponding Author: C. BOUTGHAN (email: boutaghanecherifa@yahoo.fr)

(Received: 16-March-2018; accepted: 10-July-2018; published: 20-July-2018)

DOI: <http://dx.doi.org/10.25073/jaec.201822.133>

**Abstract.** After the absorption of the photons, during the photovoltaic conversion process, one part of the radiation remains unabsorbed causing the cell to overheat and thus a drop in efficiency. The purpose of this study is to explore the effect of junction temperature, geographic coordinates as well as the season on the electrical performance of the photovoltaic cell. The results obtained show that the junction temperature has an effect which is not favorable on the electrical efficiency of the module for high temperatures around midday which is of 11% however it reaches 14% for low temperatures in the morning. Geographical coordinates at different altitudes, have no effect on the energy produced from the module, but the effect of the season on the efficiency confirms the previous results, that, the efficiency is good for low temperatures. The results are obtained by simulation, through a computer code in FORTRAN language, designed for this purpose.

## Keywords

*Modeling solar cell, photovoltaic panel, solar field.*

## 1. INTRODUCTION

Currently the use of renewable energies as an alternative source or even as a main source of energy has spread greatly, particularly in remote areas where the distribution of conventional electricity is not guaranteed. The most common primary source for the supply of renewable energy is solar energy by means of solar panels [16]. Extracting power from these resources requires further research and development to increase reliability, reduce costs (manufacturing, use and recycling) and increase energy efficiency [19].

Photovoltaic solar cells are used to convert sunlight energy into electrical energy [5]. The photovoltaic effect used in solar cells makes it possible to directly convert the light energy (photons) from the sun rays into electricity. When the photons strike a thin surface of a semiconductor material (silicon), they transfer their energy to the electrons of matter. They then move in a particular direction, creating an electrical current.

According to the literature, the effect of several parameters on the characteristic and electrical behavior of a solar cell is studied, such as the influence of solar irradiance and ambient temperature on the optimal resistance of a PV generator [17].

[6], taking into account the environmental parameters relating to illumination and ambient temperature on the characteristic behavior of the PV cell, A. Khalifa et al. [7], presents the results of his work on the effect of junction temperature (cell). The increase of the latter, which will cause the drop in the cell's electrical efficiency, is due to the part of the radiation not absorbed by the cells [7].

[8] has studied the characterization of the electrical operation of PV panels. According to these results, when the radiation varies between  $300 \text{ W/m}^2$  and  $900 \text{ W/m}^2$ , the optimum voltage decreases by 10.2%.

The work of [9] on PV modules performance degradation in the Saharan environment showed that the efficiency lost 19% of its initial value. The main objective of this work is to study the influence of the geographic coordinates and the junction temperature on the performances of a photovoltaic module and therefore provide recommendations to overcome the unfavorable effect of the latter.

## 2. MATHEMATICAL MODELING

### 2.1. System description

A photovoltaic cell, consists of two doped silicon layers, one of which has an excess of electrons (layer N) and the other has an electron deficiency (layer P). There is production of electrical energy after absorption of incident photons and creation of electron-hole pairs if the energy of the photon is greater than the gap of the material.

A panel is a series assembly of these cells. The power generated depends on the load at the panel output.

The system studied in this paper is a photovoltaic generator, Fig.1. Located at the level of the city of Constantine with the following geographical coordinates ( $6^\circ$  longitude,  $36^\circ$  latitude and 693 m of altitude) and an inclination equal the latitude of the place, composed of fifteen (15) monocrystalline modules type

"CNPV-50M", mounted in series. Each module consists of (36 cells), whose characteristics shown in table.1.



Fig. 1: General View of a photovoltaic module

### 2.2. Modeling of the solar field

The study of the solar potential is the starting point of any study concerning the dimensioning of a solar installation or of an energy system. Then, it is necessary to know the meteorological weather conditions of the site of implantation to evaluate and to estimate the solar potential [10].

In Algeria, the number of stations to assess the solar field is very limited [11]. Certain approaches are used to predict the characteristics of solar radiation [12]. Several models exist for the estimation of the different components of the global, direct and diffuse solar irradiation. Most existing models require the knowledge of a large number of site data. In Algeria, generally

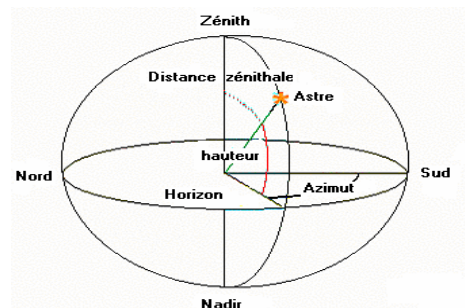


Fig. 2: Horizontal coordinates of the sun.

these data are not all available. In our study, we adopted the Kasten model [1], which is valid for heights of more than  $10^\circ$ , and considers the atmospheric disturbance [1]. Similarly, there are

Table 1. Characteristics of the photovoltaic module.

Characteristics	Unit	CNPV-50M
Nominal power $P_{max}$	Wc	50
Maximum voltage $V_{mp}$	V	19.0
Maximum current $I_{mp}$	A	2.63
Open circuit voltage $V_{oc}$	V	22.7
Short circuit current $I_{cc}$	A	2.83
Cell efficiency $\eta_c$	%	18.7
Module efficiency $\eta_m$	%	14.5
Operating temperature	°C	$45 \pm 2$
Power temperature coefficient	%/°C	-0.45

practical algorithms that allow an evaluation of the illumination received by any orientation surface from the astronomical, geographical and geometrical data of the place, Fig. 2.

Direct illumination ( $I$ ) on a horizontal plane: Direct solar radiation defined as the radiation from the solar disk alone and calculated by the expression:

$$I = I_0 \times \exp\left(-\frac{(m_h \times T_l)}{(0.9 \times m_h + 9.4)}\right) \quad (1)$$

Direct illumination on an inclined plane ( $S_i$ ):  $S_i = I \times$

$$\begin{pmatrix} \cos(h) \times \sin(i) \times \cos(a - \gamma_1) \\ + \sin(h) \times \cos(i) \end{pmatrix} \quad (2)$$

The global illumination on a horizontal plane [6]:

$$G_0 = M \times (\sin(h))^N, \quad (3)$$

where  $M, N$  : characterizing the state of the atmosphere.

Depending on the state of the sky, the global illumination is determined on a horizontal plane by one of the Following formulas [6]:

$$\text{DegradedSky} : G_0 = 990 \times (\sin(h))^{1.25} \quad (4)$$

$$\text{AverageSky} : G_0 = 1080 \times (\sin(h))^{1.22} \quad (5)$$

$$\text{PureSky} : G_0 = 1150 \times (\sin(h))^{1.15} \quad (6)$$

The diffuse illumination ( $D_0$ ) on a horizontal plane [6]:

$$D_0 = \frac{I_0}{25} \times (\sin(h))^{\frac{1}{2}} \times (T_L - 0.5 - (\sin(h))^{\frac{1}{2}}) \quad (7)$$

The diffuse illumination ( $D_i$ ) on a plane of inclination ( $i$ )

$$D_i = \left(\frac{1 + \cos(i)}{2}\right) \times D_0 + \left(\frac{1 - \cos(i)}{2}\right) \times a_1 \times G_0 \quad (8)$$

The global illumination on an inclined plane ( $G_h$ ) is given by:

$$G_h = S_i + D_i \quad (9)$$

With: The following expression, called Gauss's formula, gives the angular height of the sun [2]:

$$\begin{aligned} \sin(h) &= \sin(\delta) \times \sin(\varphi) \\ &+ \cos(\delta) \times \cos(\varphi) \times \cos(w), \end{aligned} \quad (10)$$

where

- $i$ : The inclination of the panel [°].
- $a$ : The azimuth [°].
- $\gamma_1$ : The orientation [°].
- $h$ : The height of the sun [°].
- $T_L$ : Linke's disorder factor.
- $I_0$ : Solar constant ( $I_0 = 1353 \text{ W/m}^2$ ).
- $a_1$ : the albedo (20%).
- $G_0$ : Global radiation on a horizontal plane [ $\text{W/m}^2$ ].
- $T_{max}$ : maximum daily temperature [°C].
- $T_{min}$ : minimum daily temperature [°C].

- $G_h$ : Daily solar irradiation component [W/m<sup>2</sup>].
- $n$ : Day number in the year.
- $\theta$ : Angle of incidence [°].
- $\varphi$ : The latitude [°].

where

$$\mu_T = (1 + \beta_{STC})^{(T_{cell} - T_{ref})} \quad (15)$$

$$t_m = \frac{24}{180} \times \arccos[-tg(\theta) \times tg(\varphi)] \quad (16)$$

And:

The declination ( $\delta$ ): The value of this angle can be calculated by the formula [3]:

$$\delta = 23.45 \times \sin(360 \times \frac{284 + n}{365}) \quad (11)$$

Where, ( $n$ ) is the number of the day in the year. Liu and Jordan proposed to take the 16<sup>th</sup> day of each month, as the most representative of the average day of the month considered. As for Klein he showed that it was better to choose that day using Table 2, [4]:

- $T_{cell}$ : Junction temperature [°C].
- $T_{STC}$ : temperature under reference conditions (= 25°C).
- $\beta_{STC}$ : power temperature coefficient of module in %/°C
- $\mu_T$ : Temperature correction coefficient of the cell.
- $t_m$ : Number of hours of sunshine [h].

### 2.3. Modeling of ambient temperature [18]:

$$T_a = 0,5 \times \left[ \begin{array}{l} (T_{max} + T_{min}) \\ + (T_{max} - T_{min}) \times \frac{(180 \times (t-8))}{12} \end{array} \right] \quad (12)$$

### 2.4. Modeling of junction temperature

$$T_{cell} = T_a + G_h \times \left( \frac{N_{oct} - 20}{800} \right) \quad (13)$$

where  $N_{oct}$ : Nominal cell usage temperature [°C],  $T_{cell}$ : The temperature of the cell [°C].

### 2.5. Daily energy generated

In order to evaluate the energy produced by each module, it should be reminded that the modules are classified under nominal operating conditions, but the working conditions actually recorded in the field rarely correspond to their nominal values. Thus, the daily energy produced by the photovoltaic generator can be estimated by the following equation [13]:

$$E = N_{pv} \times P_{max} \times \left( \frac{G_h}{E_{STC}} \right) \times \mu_T \times t_m \quad (14)$$

### 2.6. Electrical efficiency of the panel

The efficiency of a PV module depends on the junction temperature given by the following formula [14]:

$$\eta_{pv} = \eta_{STC} [1 - \beta_{STC} (T_{cell} - T_{STC})] \quad (17)$$

Calculations are made from an initial time ( $t_0 = 6^h.00$ ) for the day of August and ( $t_0 = 8^h.00$ ) for the days of December ( $n = 344$ ) and April ( $n = 105$ ) because of the Kesten model that is valid for Sun heights greater than (10°), and a time step equal to one hour. The results obtained by simulation and through a computer code in FORTRAN language. All the following results are about the representative day of August ( $n = 228$ ).

## 3. RESULTS AND DISCUSSION

### 3.1. Temporal evolution of solar irradiation

The observation of Fig. 3 shows that the curve representing the global radiation temporal evolution calculated by the Kasten formula is close

Table 2. Number estimation of the day of the year.

Month	$N^o$ of the day in the month	$N^o$ of the day in the year
January	17	17
February	16	47
March	16	75
April	15	105
May	15	135
June	11	162
July	17	198
August	16	228
September	15	258
October	15	288
November	14	318
December	10	344

Table 3. Below gives the characteristics of our module.

Type	Monocrystalline model CNPV-50M
maximum power (nominal)	$P_{max} = 50 \text{ Wc}$
maximum current	$I_m = 2.63 \text{ A}$
maximum voltage	$V_m = 19.0 \text{ V}$
short circuit current	$I_{cc} = 2.83 \text{ A}$
open circuit voltage	$V_{co} = 22.7 \text{ V}$
Operating temperature	NOCT = 45 °C
Reference efficiency	$\eta_{STC} = 14,5 \%$
temperature coefficient for Pmax	$\beta_{STC} = -0045/^{\circ}\text{C}$

to the curve resulting from the experiment [15]. At solar noon, the global irradiation component is of the order of 1077 W/m<sup>2</sup>. The global ir-

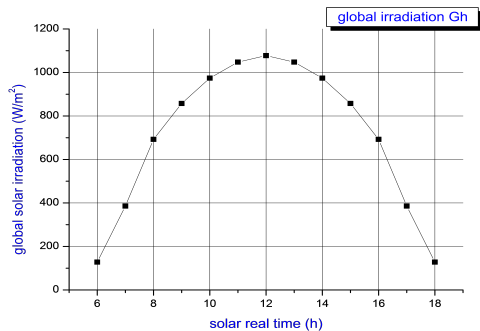


Fig. 3: Temporal evolution of the daily global irradiation for  $n = 228$  and with a pure sky.

radiation component represents the sum of the two components of radiation, the direct and the diffuse. The two figures below clearly show the validation of Kasten’s model. Figure 4 shows the temporal evolution of the two components,

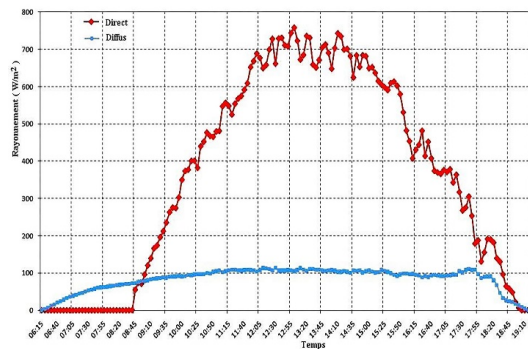


Fig. 4: Incident solar radiation on a horizontal plane 14/04/2007.

direct and diffuse on a horizontal plane resulting from the experience for the site of Ghardaïa, located in southern Algeria with the following coordinates [altitude ( $Z = 468$ ), latitude ( $\varphi = 32.40$ )]. The observation of Fig. 5, allows to notice that the curve representing the temporal evolution of direct and diffuse radiations, Calculated by Kasten’s formula, is overall close to

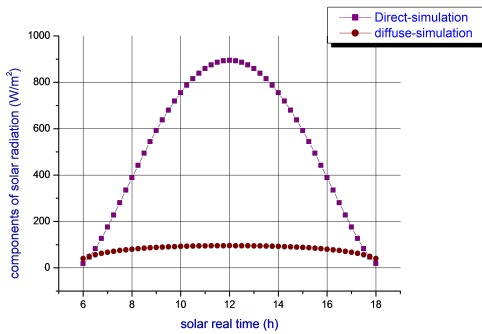


Fig. 5: Direct and diffuse component by simulation.

the curve from experience (Fig. 5); except for the direct radiation in the morning, which can be due to more precise factors and coefficients (albedo, condensable water height, etc.), which were used in the calculations.

### 3.2. Temporal evolution of ambient and cell temperatures

As shown in Fig. 6, the ambient temperature is constantly changing with time. For the cell temperature, it is higher than the ambient temperature. It has the same outline as reference [7], but we notice that it takes the shape of the component of the solar irradiation, so the latter increases as the irradiation increases, same results of the reference [8].

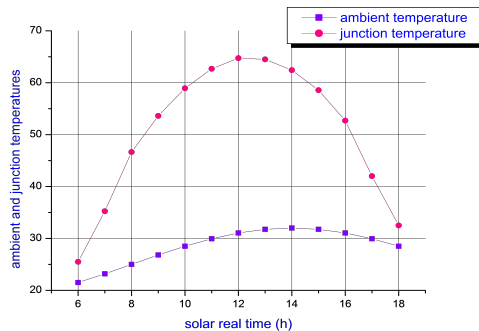


Fig. 6: Temporal evolution of ambient and junction temperatures for  $n = 228$  with a pure sky.

### 3.3. Temporal evolution of the daily energy produced by the photovoltaic generator

The analysis of the curve of Fig. 7, clearly demonstrates that the curve takes the same form as that of irradiation, which indicates that the daily energy produced by the GPV, being of the order of (8 KWh) at solar noon, is proportional to irradiation.

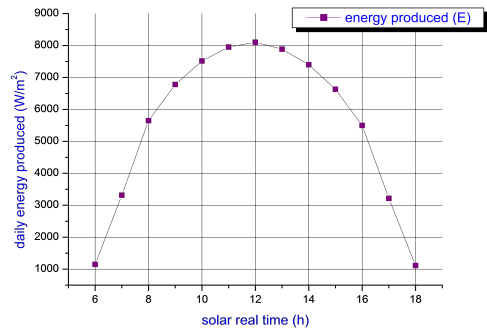
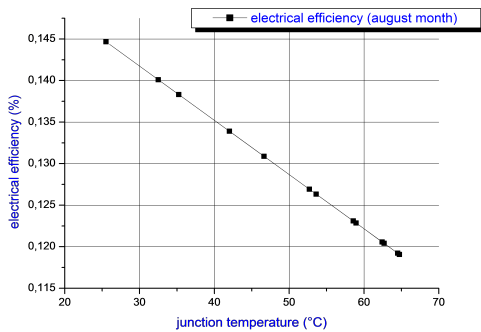


Fig. 7: Temporal evolution of the energy produced by the generator for  $n = 228$  under a pure sky.

### 3.4. Effect of cell temperature on efficiency

Figure 8 shows the evolution of the electrical efficiency. According to this figure, the electrical efficiency is inversely proportional to the junction temperature of the PV panel. Therefore, the effect of the latter is not favorable on the electrical efficiency. It is of the order of (14%) at the minimum cell temperature (25°C) to (6.00 a.m.) and of (11%) for the maximum temperature (64 °C) towards (12.00 h), close to the experimental result (10 %) of the reference [7] at solar noon. It has been shown previously that the temperature of the photovoltaic cell will rise with increasing radiation, therefore according to the literature, the more the illumination increases, the temperature of the photovoltaic cell drops and the no-load voltage ( $V_{co}$ ) falls; this induces the degradation of the performance of the photovoltaic module [8].



**Fig. 8:** Evolution of the electrical efficiency as a function of the junction temperature for  $n = 228$  and under a pure sky.

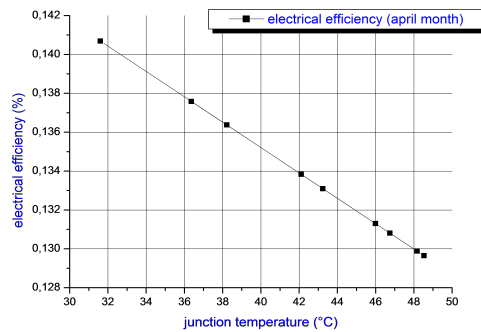


**Fig. 10:** Evolution of electrical efficiency as a function of the junction temperature for  $n = 105$  under an average sky.

### 3.5. Effect of the season on the electrical efficiency

In order to show the influence of the season, on the electrical efficiency, We have shown the evolution of the electrical efficiency as a function of the junction temperature for two months of different seasons. April ( $n = 105$ ) and December ( $n = 344$ ). The results illustrated in the two figures, Fig. 9, Fig. 10, clearly show that the efficiency towards solar noon is slightly higher in December (13%,  $T_j = 41^\circ\text{C}$ ) than in April (12%,  $T_j = 51^\circ\text{C}$ ). This confirms the previous results, that the efficiency is good for lower junction temperatures.

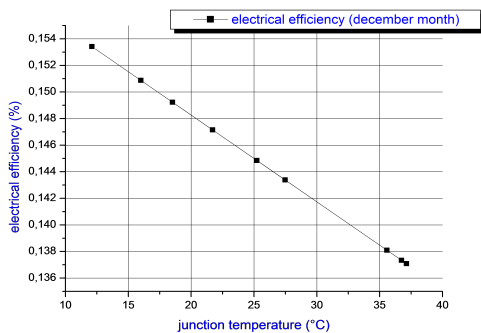


**Fig. 9:** Evolution of electrical efficiency as a function of the junction temperature for  $n = 344$  under a degraded sky.

### 3.6. Effect of geographic coordinates on energy production

We Observed in Fig. 11, that all the curves representing the temporal evolution of the energy produced by the generator for different altitudes ( $Z$ ) of the implantation site of the photovoltaic generator and for the same day in the year ( $n = 228$ ) are superimposed, indicating that the geographical coordinates have no effect on the production of daily energy.

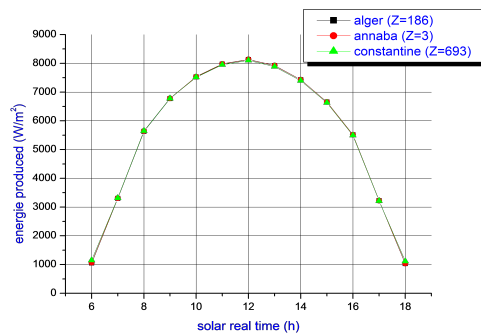


**Fig. 11:** Temporal evolution of the energy produced by the generator for different altitudes for  $n = 228$  and under a pure sky.

## 4. CONCLUSION

It is important to study the influence of the interior and exterior parameters of the photovoltaic system on these performances. According to the obtained results, the external parameter (geographical coordinates) has no effect on the electrical production and the internal parameter studied (junction temperature) has an effect that is not favorable for high temperatures on the electrical efficiency. However, the increase in irradiation has had a good effect on electrical production. Hence, the importance of lowering this temperature by cooling and adopt a hybrid system PVT, and integrate the MPPT technique into the system, in order to find the most economical system and even to value the solar electrical production.

## References

- [1] Communay, P. H. (2002). *Héliothermique: le gisement solaire, méthodes et calculs*. Groupe de recherche et d'édition.
- [2] Bernard, J. (2011). *Energie solaire: calculs et optimisation*. Ellipses.
- [3] Bernard, R., Menguy, G., & Schwartz, M. (1980). *1980-Le Rayonnement Solaire: Conversion Thermique et Application*. Technique et Documentation, Paris, 215p.
- [4] Daguene, M. (1985). *Les séchoirs solaires*.
- [5] Touafek, K., Haddadi, M., Malek, A., & Bendaikha-Touafek, W. (2008). Simulation numérique du comportement thermique du capteur hybride solaire photovoltaïque thermique. *Revue des énergies renouvelables*, 11(1), 153-165.
- [6] Belhaouas, N., Cheikh, M. A., Malek, A., & Larbes, C. (2013). Matlab-Simulink of photovoltaic system based on a two-diode model simulator with shaded solar cells. *Revue des Energies Renouvelables*, 16(1), 65-73.
- [7] Khelifa, A., & Touafek, K. (2012). Etude de l'influence des paramètres externes et internes sur le capteur hybride photovoltaïque thermique (PVT). *Revue des Energies Renouvelables*, 15(1), 67-75.
- [8] Mrabti, T., El Ouariachi, M., Tidhaf, B., & Kassmi, K. (2009). Caractérisation et modélisation fine du fonctionnement électrique des panneaux photovoltaïques. *Revue des Energies Renouvelables*, 12(3), 489-500.
- [9] Sadok, M., Benyoucef, B., & Mehdaoui, A. (2012). Performances et Dégradation des Modules PV en milieu saharien. *Revue des Energies Renouvelables, SIENR*, 12, 203-212.
- [10] Hamdani, M., Bekkouce, S. M. A., Benouaz, T., & Cherier, M. K. (2011). Etude et modelisation du potentiel solaire adequat pour l'estimation deseclairements incidents a Ghardaia. *Revue internationale d'héliotechnique*, (43), 8-13.
- [11] Mefti, A., Bouroubi, M. Y., & Khellaf, A. E. (1999). Analyse critique du modèle de l'atlas solaire de l'Algérie. *Rev. Energ. Ren*, 2, 69-85.
- [12] Gairaa, K., & Benkacali, S. (2008). Modélisation numérique des irradiations globale et diffuse au site de Ghardaïa. *Revue des Energies Renouvelables*, 11(1), 129-136.
- [13] Fortunato, B., Torresi, M., & Deramo, A. (2014). Modeling, performance analysis and economic feasibility of a mirror-augmented photovoltaic system. *Energy Conversion and Management*, 80, 276-286.
- [14] Ibrahim, A., Fudholi, A., Sopian, K., Othman, M. Y., & Ruslan, M. H. (2014). Efficiencies and improvement potential of building integrated photovoltaic thermal (BIPVT) system. *Energy Conversion and Management*, 77, 527-534.
- [15] Gama, A., Haddadi, M., & Malek, A. (2008). Etude et réalisation d'un concentrateur cylindro parabolique avec poursuite solaire aveugle. *Revue des énergies renouvelables*, 11(3), 437-451.

- [16] Recherches en cours du professeur Kodjo Agbossou. (Report)
- [17] Hamidat, A., Chouder, A., Benyoucef, B., Belhamel, M., Tchikou, A., & Guilane, K. (2003). Conception et Réalisation d'un Système de Chauffe-eau Solaire Photovoltaïque. *Revue des énergies renouvelables*, 33-38.
- [18] Zarai, N., Chaabane, M., and Gabsi, S. (2010). Planification de la Production Thermique des Capteurs Solaires. International Renewable Energy Congress, Sousse, Tunisia.
- [19] Baghdadi fazia. Modélisation et Simulation des Performances d'une Installation Hybride de Conversion d'Energie Renouvelables. Département de génie mécanique, Université Mouloud Mammeri, Tizi-Ouzou. Thèse de magistère (2011). (Theses (M.S.) and Dissertations (Ph.D.))

"This is an Open Access article distributed under the terms of the Creative Commons Attribution License, which permits unrestricted use, distribution, and reproduction in any medium, provided the original work is properly cited (CC BY 4.0)."